Evaluation of Cathodic Assemblages and Monitoring Devices for a Bioelectrochemical Slurry Reactor Treating a Soil Polluted with Lindane

Ricardo H. Blanco-Mendoza, **Héctor M. Poggi-Varaldo** (r4cepe@yahoo.com), Rafael Hernández-Vera, and E. Hernández-Correa (CINVESTAV, Mexico City, Mexico)
Noemi Rinderknecht-Seijas (ESIQIE-IPN, Mexico City, Mexico)
Beni Camacho-Pérez (University of Tecamac, Mexico)

ABSTRACT: The objectives of this work were three-fold: *(i)* to evaluate the effect of cathode-membrane assemblage, conventional and new, on electrochemical variables of a bioelectrochemical continuous slurry reactor (*BECSR*) during its batch operation; *(ii)* to determine the suitability of monitoring *BECSR* potential with a low cost instrument instead a standard, more expensive multimeter; and *(iii)* to evaluate environmental performance of the *BECSR* loaded with a heavy soil polluted with 100 mg lindane/kg soil. The *BECSR* was operated in 30 d batch mode. At day 0, internal resistances of the conventional and new cathodic assemblages were 3300 and 5800 Ω, respectively. At day 7, new polarization curves showed that internal resistances significantly decreased for both types of assemblages attaining values of 440 and 450 Ω, respectively. Electrochemical performance of the *BECSR* equipped with conventional cathodic assemblage was similar or slightly superior to that of the new assembles (considering the 30 d of operation), in terms of both higher average E and volumetric powers. Yet, in the last subperiod of operation from day 21 to the 30th day, the new assemblage performed better than the conventional one. Fabrication of the conventional cathodic assemblage resulted less expensive and less time consuming. Comparison between monitoring devices showed that the expensive Escort multimeter can be replaced by a very low cost device Arduino to monitor potential of *MFC*s because their potential readings were very close, practically equal; cost savings represent ca. 99%. Thus, conventional assemblage was selected for future construction of other *BECR*s. Removal of lindane was moderate (60%), slightly lower than lindane removals obtained in slurry bioreactors operated either as aerobic or sulphate-reducing modes.

Keywords: Arduino UNO, Bioelectrochemical Slurry Reactor, Conventional Assemblage membrane-cathode, Lindane, New Assemblage membrane-cathode.

INTRODUCTION

Microbial fuel cells (*MFC*) constitute a promising technology for sustainable remediation of polluted soils and waters (Poggi-Varaldo et al. 2009; Poggi-Varaldo et al. 2010). *MFC* belong to the now extended family of bioelectrochemical systems (BES). Typically, two broad types of *BES* are distinguished: *(i)* microbial fuel cell *MFC*, that use a microbial culture to oxidize organic matter, harvest electrons and transfer the electrons to the anode that is externally connected to the cathode, generating an electric current. Once in the cathode, the electrons are transferred to a terminal electron acceptor, like oxygen or another oxidized compound; and *(ii)* microbial electrolysis cells (*MEC*), that utilize an external electrical energy input to perform in a variety of applications, from gas biofuels production to microbial electrosynthesis of value-added compounds (Liu *et al.* 2013; Hernández-Correa *et al.*, 2017).

Regarding *MFC* they exhibit a crucial advantage: they can use effluents (wastewaters or contaminated groundwaters, as well as other low-grade biomass) to produce bioelectricity and simultaneously abating the pollutant load of the liquid or soil

matrices (Camacho-Pérez *et al.*, 2013; Zhou *et al.* 2013). The application of *MFC* to soil/sediment remediation has led to the development of the bioelectrochemical slurry reactor (*BECSR*, also known as Soil microbial fuel cell *SMFC*), i.e., a hybrid of *MFC* and slurry bioreactors (Camacho-Pérez *et al.*, 2013). There is an increased interest on the application of *BECSR* to the remediation of soils polluted with a great variety of contaminants, spanning from lindane to oils hydrocarbons, passing through phenols and chlorophenols (Camacho-Pérez *et al.*, 2013; Sánchez-López *et al.*, 2017).

Typically, cell portential *E* is the main variable monitored for determining *BECSR* I performance. Other variables such as cell power *P* and current intensitiy *I* can be easily derived by using the potential and the external resistance(Logan *et al.* 2006; Poggi-Varaldo *et al.* 2010) based on Ohm's law for direct current circuits, i.e.

$$I = E / R_{ext} \hspace{4cm} [1]$$

$$P = E^2/R_{ex} \hspace{4cm} [2]$$

where *E* is the potential measured cell potential, R_{ext} is the external resistance.

Average quantities of *I* and *P* can be estimated by numerical integration of P and I over the time of cell operation (suitably subdivided in small intervals, and using Simpson rule, for instance), and futher dividing the obtained charge or the obtained energy by the overall time of operation.

Bioelectrochemical device experiments face very often the limitation of monitoring instrumentation that can be very expensive (typically potential monitoring multimeters coupled to computers for automatic registration of the readings, or potentiometers). Particularly, this is a systemic problem in underdeveloped countries, where budgets for research and development are usually very low.

In this work, we explored the application of a low-cost microcontroller board "Arduino UNO" for such task. The Arduino UNO is an open-source platform with its own compiler that uses simplified C++ language. The devices have several advantages, inter alia: *(i)* code and data acquisition via USB cable are easy to load and operate, *(ii)* the device has multiple analog ports for multiple, simultaneous potential readings, and *(iii)* the low cost of the board (pricing around 20 $USD in Mexico). However, the device has only 10 bits of resolution for analog to digital conversion. Therefore, we need to test the equivalence between Arduino's potential readings and those of the commercial multimeter. If equivalent, then it will be he feasible to replace expensive multimeters or potentiometers with Arduino UNO.

The *BECSR* usually consists of an anodic chamber where a suspension of the polluted soil is loaded. The cathode can be aerated (open to the atmosphere) or submerged in a cathodic chamber where oxygen is being supplied. It has been reported that by increasing the liquid (water) proportion in the soil suspension in the anode, the lower will be the internal resistance contributed by the soil (Domínguez-Garay *et al.* 2013). However, there is a practical limit to increasing water proportion in the soil suspension because the *BECSR* would be underutilized. Typically, *BECSR* operate with 25 to 40% of soil in water (w/v) in the anodic chamber. Higher proportions of soil would compromise mixing effectiveness and lead to poor *BECSR* performance. Even in the range 25-40% soil in water, the soil greatly contributes to the internal resistance of the device, and this, in turn, could translate into low bioelectricity generation. (Morris & Jin 2012; Li *et al.* 2016). Therefore, it is of outmost interest that the contribution to cell internal resistance by the assemblage membrane-cathode be minimized. We have worked with an open cathode

BECSR, where the membrane was painted and pasted to the carbon cloth that acted as the cathode. This cloth was in direct contact with atmospheric air in the extreme sides of the *BECSR* thus allowing the O2 transport. Another membrane-cathode assemblage was developed and successfully tested in hydrogen fuel cells (Solorza-Feria, private communication, 2016) where the standard carbon cloth was replaced by another type of carbon fabric with a face with micropores, among other features.

Thus, the objectives of this work were three-fold: *(i)* to evaluate the effect of cathode-membrane assemblage, conventional and new, on electrochemical variables of *BECSR* during its batch operation; *(ii)* to determine the suitability of monitoring *BECSR* potential with a low-cost instrument instead of a standard, more expensive multimeter; and *(iii)* to evaluate environmental performance of the *BECSR* loaded with a heavy soil polluted with 100 mg lindane/kg soil.

To the best of our knowledge, this is the first time that a low-cost device was tested for cell voltage monitoring in a *BECSR* and shown that can replace the more expensive multimeter.

MATERIALS AND METHODS

Experimental Design. We carried out a 2^2 factorial design. The factors were the cathode assemblage (conventional and new), and the monitoring device for the *BECSR* potential (Arduino UNO and multimeter Escort 3146A). The *BECSR* was loaded with 100 g of soil polluted with 100 mg lindane/kg dry soil and 200 mL of water with 1.2, 2.5, 0.6 g/L of $NaHCO_3$, Na_2CO_3, and $(NH_4)_2HPO_4$ respectively, the *BECSR* was batch operated with initial spiking of soluble, degradable organic matter (0.5, 0.5, and 0.5 g/L of acetate, lactate, and sucrose, respectively). Results were analyzed by statistical procedures *ANOVA* and tests of hypothesis for means of matched (paired) samples (Kreyszig 1970; Daniel 2009). The response variables analyzed were potentials (period 0-30 d; period 21-30 d) and volumetric power (period 21-30 d).

The *BECSR* was operated in batch mode for 30 d at room temperature and 100 rpm orbital agitation. At the start and 7th day, electrochemical characterization of the *BECSR* were carried out according to the polarization curve method (Poggi-Varaldo *et al.*, 2009). At day 9 of operation, the *BECSR* was fed with 10 mL of a stock solution containing 0.5, 0.5, and 0.5 g/L of acetate, lactate, and sucrose, respectively.
Potential of the *BECSR* was monitored in both assemblages every 15 min using two different devices, namely Arduino UNO and multimeter Escort 3146 A. Both assemblages were connected to both devices.

Bioelectrochemical Slurry Reactor Architecture. *BECSR* consisted of a Plexiglass cylinder approximately 7 cm in diameter and 8 cm in height, fitted with two anodes and two cathodes (Blanco-Mendoza, 2017).

The anodes were graphite discs (5cm D x 0.5 cm) whereas the cathodes were assembled with 2 different methods, and the cathode is an air-cathode. *BECSR* was inoculated with a sulfate-reducing inoculum (Blanco-Mendoza, 2017).

Conventional Assemblage. The conventional cathode assemblage consisted of a standard carbon cloth (*CC*) and a Nafion membrane; the latter was painted with a suspension of Pt (that would lead to 0.5 mg Pt/cm^2) and pressed at 40 kgf/cm^2 and 120°C for 2 min; the whole process lasted 1 d.(Vázquez-Larios et al. 2011; Camacho-Pérez et al. 2013; Hernández-Flores et al. 2015)

New Assemblage. The new assemblage consisted of a special *CC* with one side made of a layer of carbon micropores that was painted with mixture containing Pt that lead to 0.5 mg Pt/cm^2. Afterwards, the painted *CC* and the Nafion membrane were pressed together at 40 kgf/cm^2 and 120°C for 2 min. The whole procedure lasted 3 d and the special *CC* carbon cloth with a side of micropores is more expensive than the standard *CC* (Solorza-Feria, 2016, private communication).

Soil Characteristics. The soil was sampled from an agricultural field in Huajuapan de León, Oaxaca, México. Its pH was 6.64 and the soil had high contents of organic matter (12.35%). It contained 34.44% sand, 27.52% silt, and 38.04% clay. Texture results were consistent with a clayish soil. High contents of both clay and organic matter are known to be obstacles for efficient bioremediation of soils (Robles-González *et al.* 2012); bioavailability of pollutants is very low because the contaminants can be strongly attached to particles of clay and organic matter.

Data analysis. The collected data during the operation of the cell was evaluated with different statistical parameters. Absolute and relative errors (e_{abs} and e_{rel}, respectively) were estimated with Equations 3 and 4:

$$e_{abs} = |E_{Arduino} - E_{mult}| \qquad [3]$$

$$e_{rel}(\%) = \frac{|(E_{Arduino} - E_{mult})|}{E_{mult}} \times 100 \qquad [4]$$

where E_{mult} is the voltage reading of the multimeter at any specific time and $E_{Arduino}$ is the potential reading with the Arduino UNO at the same time.

The average absolute error was estimated with Eq 5 below:

$$\bar{e}_{Abs} = \frac{1}{N}\Sigma|(E_{Arduino} - E_{mult})| \qquad [5]$$

where N is the total number of readings.

Average voltages were estimated as usual:

$$\bar{E}_{Arduino} = \frac{1}{N}\Sigma_1^N E_{Arduino} \qquad [6\ a]$$

$$\bar{E}_{mult} = \frac{1}{N}\Sigma_1^N E_{mult} \qquad [6\ b]$$

The norm, that is a primary fitting parameter is given by Eq 7

$$Norm = \Sigma_1^N(E_{Arduino} - E_{mult})^2 \qquad [7]$$

The error variance σ_e^2, standard deviation σ_e of the error, and variation coefficient were calculated as follows:

$$\sigma_e^2 = \frac{1}{N-1}\Sigma(E_{Arduino} - E_{mult})^2 \qquad [8]$$

$$\sigma_e = \sqrt{\sigma_e^2} \qquad\qquad [9]$$

$$CVar_e = \left(\frac{\sigma_e}{\bar{E}}\right) x\ 100 \qquad\qquad [10]$$

We defined a magnitude called "divergence" to be used for the test of means of matched or paired samples:

$$d = E_{Arduino} - E_{mult} \qquad\qquad [11]$$

The average of this magnitude was

$$\bar{d} = \frac{1}{N}\Sigma(E_{Arduino} - E_{mult}) \qquad\qquad [12]$$

Apart from the descriptive statistics, a hypothesis test of means (for matched or paired samples) was applied, using either α = 0.99 or 0.95, namely

Null hypothesis, $\qquad$ $H_0: \bar{d} = 0$ $\qquad\qquad$ [13 a]

Alternative hypothesis, $\quad$ $H1: \bar{d} \neq 0$ $\qquad\qquad$ [13 b]

We used the test statistic Z_{exp} (standardized Gaussian statistic) estimated with the following equation:

$$Z_{exp} = \frac{\bar{d} - 0}{\sigma_d / \sqrt{N}} \qquad\qquad [14]$$

RESULTS AND DISCUSSION

Electrochemical characterization of BECSR using polarization curve method (0 and 7 d). Figure 1 shows the polarization (red) and volumetric power (black) curves obtained at 0 and 7th day, as well as the regression based on the polarization curve (insets, *E* vs. *I*) that lead to the determination of the internal resistance R_{int} of the cell as the slope of the regression. More complete data (with maximum values of several electrochemical variables) are displayed in Table 1.

At day 0, internal resistances of the conventional and new cathodic assemblages were 3370 and 5860 Ω, respectively. This also reflected in higher volumetric power of the conventional assemblage (Table 1). Thus, at the start-up, the conventional assemblage showed the distinct advantage of a significantly lower R_{int} and higher $P_{v,max}$ than the new assemblage.

At day 7, new polarization curves showed that internal resistances significantly decreased for both types of assemblages attaining R_{int} values of 438 and 453 Ω for the, respectively. Yet, values a day 7 were very close, only slightly lower for the conventional assemblage. Decrease of R_{int} of a *MFC* after start-up has also been observed in other works (Camacho-Pérez *et al.,* 2013). It has been attributed to an in-cell acclimation/enrichment processes (Lu *et al.* 2009) due to selective pressures on the microbial community anchored in the *MFC* (both biofilm and planktonic microbes). Overall, electrochemical characteristics of both assemblages improved at 7th d compared to start-

up conditions. Also, differences on electrochemical characteristics at 7th d between assemblages were very small.
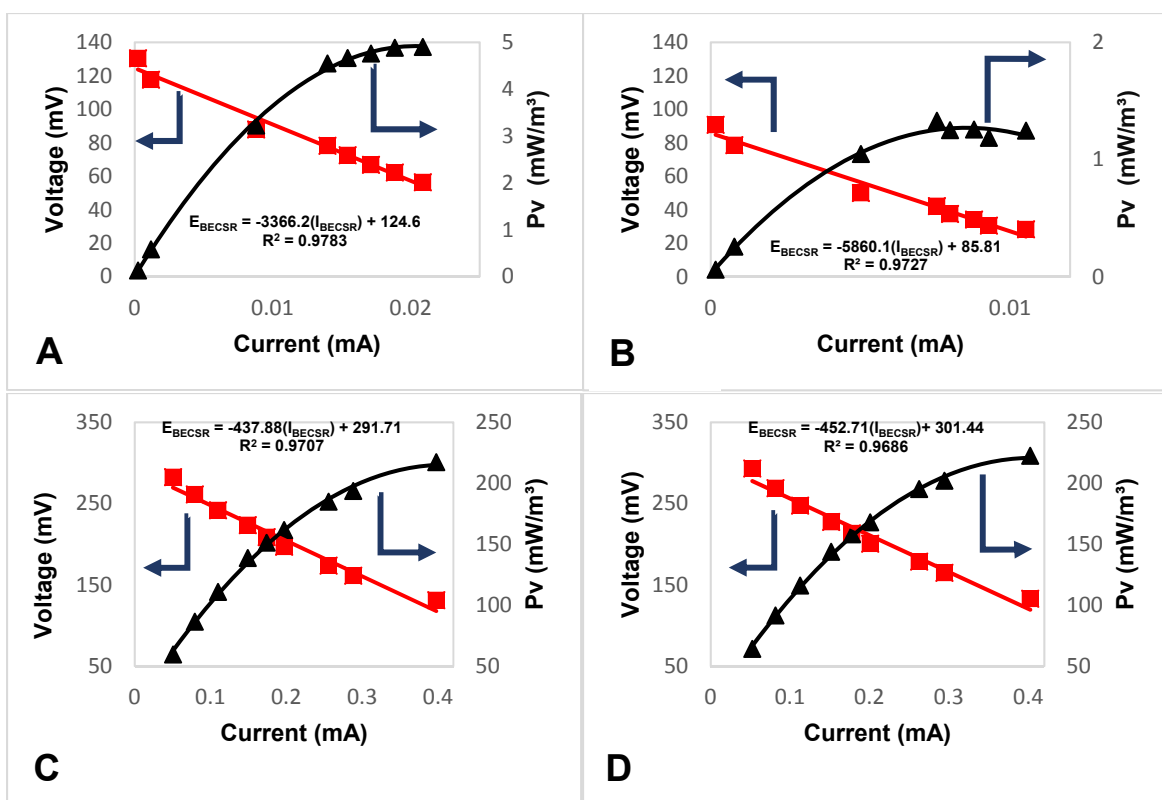
FIGURE 1. Electrochemical characterization of BECSR: (A) conventional assemblage 0 d; (B) new assemblage 0 d; (C) conventional assemblage 7 d; and (D) new assemblage 7 d.

TABLE 1. Electrochemical characterization values of the bioelectrochemical continuous slurry reactor, both assemblages in 0 and 7 d. Face A: conventional assemblage, Face B: new assemblage.

Variable	Face A 0 d	Face A 7 d	Face B 0 d	Face B 7 d
R_{int} (Ω)[a]	3300 ± 269	440 ± 8	5800 ± 99	450 ± 2
P_{An-max} (mW/m^2)[b]	0.23 ± 0.63	13.27 ± 4.50	0.076 ± 0.264	13.60 ± 2.35
$P_{v-max.}$ (mW/m^3)[c]	4.91 ± 9.62	217.21 ± 73.65	1.33 ± 4.36	222.51 ± 38.43
$P_{BECSR-max.}$ (mW)[d]	0.0012 ± 0.0023	0.0521 ± 0.0177	0.0003 ± 0.0065	0.0531 ± 0.0092
$I_{BECSR-max.}$ (mA)[e]	0.0208 ± 0.0139	0.3975 ± 0.0608	0.0075 ± 0.0239	0.4023 ± 0.0328
$E_{BECSR-max.}$ (mV)[f]	56.35 ± 37.58	131.16 ± 20.07	42.30 ± 40.96	132.75 ± 10.84

Notes: [a] Internal resistance of bioelectrochemical continuous slurry reactor. [b] Maximum anodic power density. [c] Maximum volumetric power. [d] Maximum power. [e] Maximum current intensity. [f] Potential value.

Electrochemical performance during the 30 d operation. Potential and P_v time courses are shown in Figures 2 and 3 below. The 30 d operation was subdivided in 6 stages, and average performances for all the stages are displayed in Table 2.

In stage 4, in spite of high fluctuations, the conventional assemblage was superior to the new one. After declining of fluctuations of potential to background potentials of 30 mV (end of stage 4), potentials of both assemblages started to slowly but steadily increase (stages 5 and 6, Figures 2 and 3). At the end of the operation (stage 6), the new assemblage showed a performance superior to that of the conventional one.

The electrochemical performance of our *BECSR* was in the high side of the range of electrochemical results reported in the open literature (Table 3).

Evaluation of the effect of assemblages. The results of the potentials of assemblages in the 30 d batch operation were processed according to an analysis of variance (*ANOVA*) of 2^2 experiment (Table 3A). Since this *ANOVA* reflects the effects of both factors, it can be also used for concluding about the equivalence of Arduino and multimeter for monitoring voltages. According to Table 4A, neither factor was significant. Therefore, based on the *ANOVA* results, assemblages were equivalent and consequently, the more economic Arduino can replace the more expensive multimeter as potential monitoring device.

Interestingly, regarding the last 9 days of operation (21 to 30 d) the new assemblage was superior to the conventional one (both in potential and volumetric power Tables 4B and 4B), although this pattern did not offset the superior performance of the conventional assemblage in Stage 4.

We applied another statistical tool for the analysis of the Assemblage results. It consisted of a hypothesis test of paired potential results for the whole period of operation 0-30 d. (Kreyszig 1970; Daniel 2009) (Table 4). Results show that the average deviation d bar was positive, i.e., 6.82 mV.

For this test, d was defined as $d = E_{conv.\ assemblage} - E_{new\ assemblage}$ (Table 5), it is a first indication that $E_{conv.\ assemblage} > E_{new\ assemblage}$

Actually, the null hypothesis of equal potentials should be rejected because the experimental statistic Z_{exp} = 5.42 lies out of the acceptance regions of the null hypothesis -1.96 < Z < 1.96 (alpha = 0.05) or -2.576 < Z < 2.576 (alpha = 0.01).

That is, $E_{conventional\ assemblage} \neq E_{new\ assemblage}$ (the alternative hypothesis) is valid, and because of the positive sign of d, it follows that $E_{conventional\ assemblage} > E_{new\ assemblage}$.

Going back to the whole period of operation of 30 d, not only the average potential of the conventional assemblage was superior to the new one; also the time for preparing the conventional assemblage as well as the cost (see detailed discussion on costs below) were ca. 70% shorter and lower than those of the new assemblage. So, there is no evidence to replace the conventional assemblage by the new one.

Cost analysis between conventional assemblage and new assemblage. The assemblages differed at least in two aspects: *(i)* Surface area concentration of the catalyst was 0.50 and 0.55 mg Pt/cm^2 for the conventional and new assemblage, respectively. The new assemblage received a 10% excess of Pt to compensate for catalyst losses and deterioration (Solorza-Feria, private communication, 2017). So the cost of catalyst paint and liquid Nafion were 0.88 and 1.13 USD for the conventional and new assemblages, respectively; *(ii)* the standard carbon cloth of the conventional assemblage is less expensive than the microporous carbon cloth of the new assemblage, 1.35 and 8.17 USD, respectively, for an electrode surface area of 38.48 cm^2. Prices of the components were obtained from www.fuelcellsetc.com and www.fuelcellstore.com.

According to the above discussion, the costs (on the basis of electrode area of 38.48 cm^2) were 2.2 and 9.30 USD for the conventional and new assemblage, respectively. The new assemblage is *ca.* 7.1 USD more expensive that the conventional one, that is, by a factor of 4.2 or approximately 323% higher.
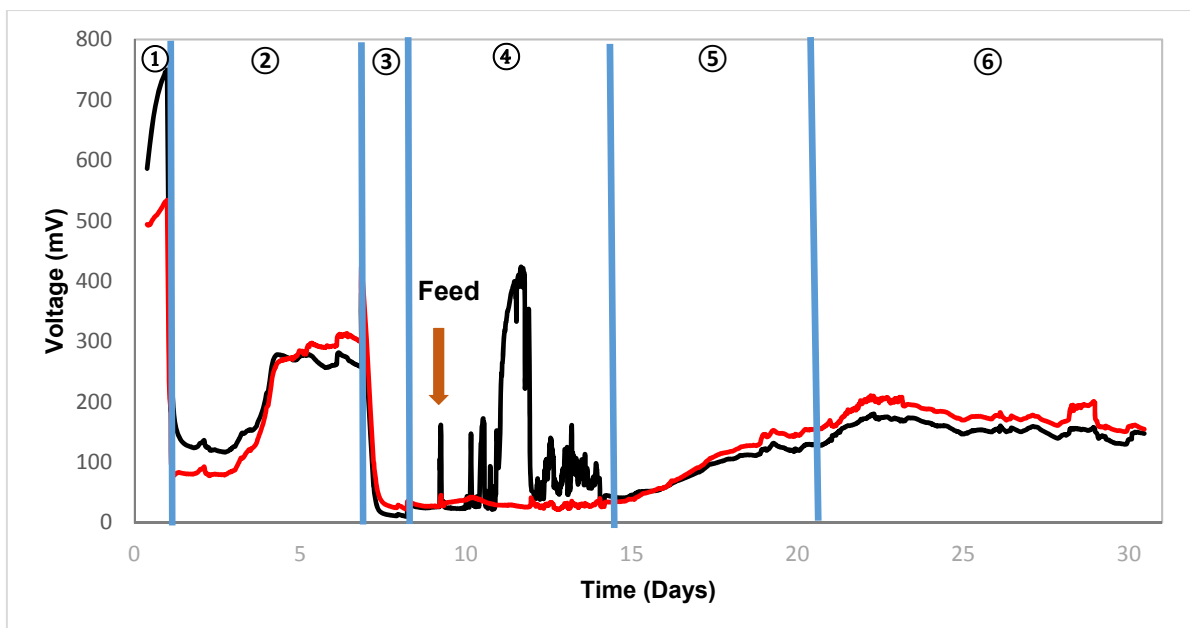
FIGURE 2. Potential time course of BECSR during 30 d of operation. The black line is the conventional assemblage and the red line is the new assemblage. The orange arrow is the substrate addition. Stage 1, open circuit; Stage 2, external resistance 2700 Ω in phase A and 5600 Ω in phase B; Stage 3, external resistance 100 Ω in phase A and 330 Ω in phase B; Stage 4, external resistance 330 Ω in phase A and 560 Ω in phase B; Stage 5, external resistance 560 Ω in phase A and 680 Ω in phase B; Stage 6, external resistance 680 Ω in phase A and 680 Ω in phase B.
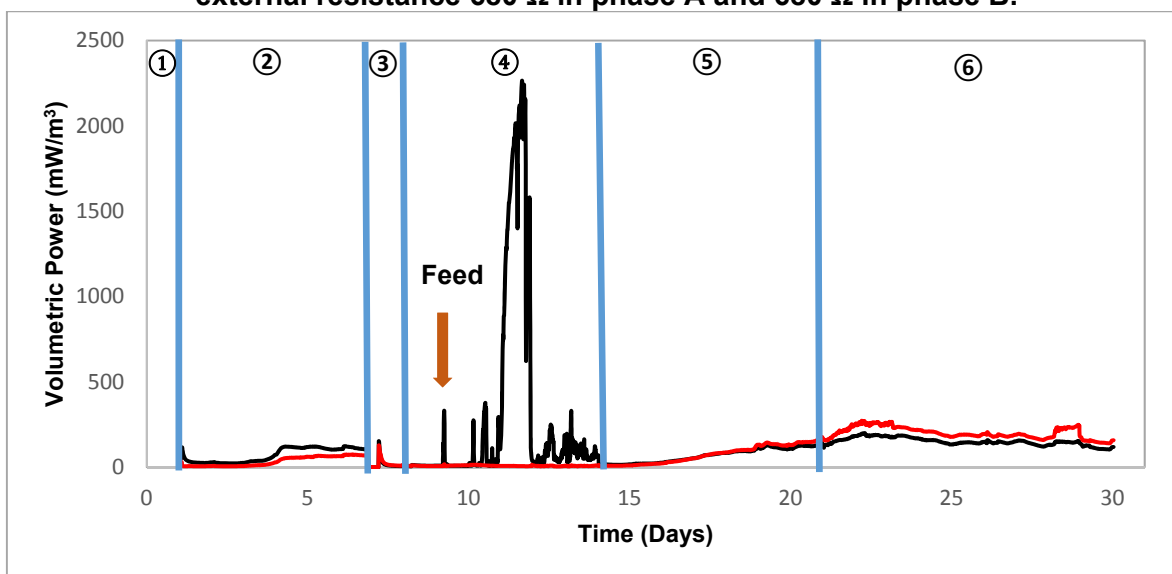
FIGURE 3. Volumetric power time course of BECSR during 30 d of operation. The black line is the conventional assemblage and the red line is the new assemblage. The orange arrow is the substrate addition. Stage 1, open circuit; Stage 2, external resistance 2700 Ω in phase A and 5600 Ω in phase B; Stage 3, external resistance 100 Ω in phase A and 330 Ω in phase B; Stage 4, external resistance 330 Ω in phase A and 560 Ω in phase B; Stage 5, external resistance 560 Ω in phase A and 680 Ω in phase B; Stage 6, external resistance 680 Ω in phase A and 680 Ω in phase B.

TABLE 2. Electrochemical parameters (maxima and average) of the six stages or periods of operation of the *BECSR*.

Etapa	Parameter	Face A (conventional assemblage)	Cara B (new assemblage)
1	$E_{BECSR\text{-máx.}}$ (mV) [a] $E_{BECSR\text{-prom.}}$ (mV) [b]	750.20 691.11 ± 48.38	533.14 511.19 ± 13.28
2	$E_{BECSR\text{-max.}}$ (mV)[a]	280.87	313.52
	$P_{An\text{-max.}}$ (mW/m^2)[c]	7.39	4.46
	$P_{v\text{-max.}}$ (mW/m^3)[d]	121.25	75.83
	$P_{BECSR\text{-max.}}$ (mW)[e]	0.0291	0.0182
	$I_{BECSR\text{-max.}}$ (mA)[f]	0.1040	0.0559
	$E_{BECSR\text{-ave.}}$ (mV)[b]	204.18 ± 66.31	190.44 ± 96.69
	$P_{An\text{-ave}}$ (mW/m^2)[g]	4.13 ± 2.73	2.18 ± 1.60
	$P_{v\text{-ave}}$ (mW/m^3)[h]	67.53 ± 44.64	35.65 ± 26.09
	$P_{BECSR\text{-ave}}$ (mW)[i]	0.0162 ± 0.0107	0.0086 ± 0.0063
	$I_{BECSR\text{-ave}}$ (mA)[j]	0.0720 ± 0.0286	0.0357 ± 0.0158
3	$E_{BECSR\text{-max.}}$ (mV)[a]	23.28	50.43
	$P_{An\text{-max.}}$ (mW/m^2)[c]	0.45	0.63
	$P_{v\text{-max.}}$ (mW/m^3)[d]	7.50	10.42
	$P_{BECSR\text{-max.}}$ (mW)[e]	0.0018	0.0025
	$I_{BECSR\text{-max.}}$ (mA)[f]	0.1325	0.0866
	$E_{BECSR\text{-ave.}}$ (mV)[b]	16.77 ± 10.21	35.03 ± 17.66
	$P_{An\text{-ave}}$ (mW/m^2)[g]	0.96 ± 1.62	1.17 ± 1.52
	$P_{v\text{-ave}}$ (mW/m^3)[h]	15.65 ± 26.48	19.14 ± 24.79
	$P_{BECSR\text{-ave}}$ (mW)[i]	0.0038 ± 0.0064	0.0046 ± 0.0059
	$I_{BECSR\text{-ave}}$ (mA)[j]	0.1677 ± 0.1021	0.1061 ± 0.0535
4	$E_{BECSR\text{-max.}}$ (mV)[a]	423.44	42.35
	$P_{An\text{-max.}}$ (mW/m^2)[c]	138.39	0.82
	$P_{v\text{-max.}}$ (mW/m^3)[d]	2,263.91	13.34
	$P_{BECSR\text{-max.}}$ (mW)[e]	0.5433	0.0032
	$I_{BECSR\text{-max.}}$ (mA)[f]	1.2832	0.0756
	$E_{BECSR\text{-ave.}}$ (mV)[b]	101.00 ± 114.58	30.60 ± 4.54
	$P_{An\text{-ave}}$ (mW/m^2)[g]	18.00 ± 36.31	0.44 ± 0.13
	$P_{v\text{-ave}}$ (mW/m^3)[h]	294.48 ± 594.02	7.12 ± 2.19
	$P_{BECSR\text{-ave}}$ (mW)[i]	0.0707 ± 0.1426	0.0017 ± 0.0005
	$I_{BECSR\text{-ave}}$ (mA)[j]	0.3061 ± 0.3472	0.0546 ± 0.0081
5	$E_{BECSR\text{-max.}}$ (mV)[a]	137.81	169.23
	$P_{An\text{-max.}}$ (mW/m^2)[c]	8.64	10.72
	$P_{v\text{-max.}}$ (mW/m^3)[d]	141.13	175.42
	$P_{BECSR\text{-max.}}$ (mW)[e]	0.0339	0.0421
	$I_{BECSR\text{-max.}}$ (mA)[f]	0.2462	0.2486
	$E_{BECSR\text{-ave.}}$ (mV)[b]	91.08 ± 31.79	101.60 ± 43.22
	$P_{An\text{-ave}}$ (mW/m^2)[g]	4.23 ± 2.53	4.56 ± 3.17
	$P_{v\text{-ave}}$ (mW/m^3)[h]	69.23 ± 41.36	74.66 ± 57.79
	$P_{BECSR\text{-ave}}$ (mW)[i]	0.0166 ± 0.0099	0.0179 ± 0.0124
	$I_{BECSR\text{-ave}}$ (mA)[j]	0.1626 ± 0.0568	0.1494 ± 0.0636

6			
	$E_{BECSR-max.}$ (mV)[a]	175.06	207.51
	$P_{An-max.}$ (mW/m^2)[c]	11.49	16.12
	$P_{v-max.}$ (mW/m^3)[d]	187.92	263.75
	$P_{BECSR-max.}$ (mW)[e]	0.0451	0.0633
	$I_{BECSR-max.}$ (mA)[f]	0.2568	0.3046
	$E_{BECSR-ave.}$ (mV)[b]	155.52 ± 11.94	179.51 ± 15.28
	P_{An-ave} (mW/m^2)[g]	9.11 ± 1.39	12.16 ± 2.06
	P_{v-ave} (mW/m^3)[h]	149.07 ± 22.66	198.87 ± 33.72
	$P_{BECSR-ave}$ (mW)[i]	0.0358 ± 0.0054	0.0477 ± 0.0081
	$I_{BECSR-ave}$ (mA)[j]	0.2287 ± 0.0176	0.2639 ± 0.0225

Notes: [a] Maximum potential value. [b] Average voltage. [c] Maximum anodic power density. [d] Maximum volumetric power. [e] Maximum power. [f] Maximum current intensity. [g] Average anodic power density. [h] Average volumetric power. [i] Average power. [j] Average current intensity.

Evaluation of the feasibility of replacing multimeter by Arduino UNO. First, Figure 4 shows the comparison one-to-one of the potentials read in Arduino and multimeter. From this simple graphic, It can be seen that results Arduino and multimeter potentials were very close. The regressions of potentials exhibited slope values close to 1, the divergence of the slopes was 1% at most (see insets in Figure 4).

A thorough data analysis (with calculations of absolute and relative errors, among others) of the evaluation of the possible equivalence of the potentials obtained with Arduino UNO and the multimeter Escort is depicted in Tables 6 and 7, for conventional and new assemblages, respectively.

Absolute and relative (average) errors between readings of Arduino and multimeter were very low for both assemblages. Errors were slightly lower for the results of the conventional assemblage (Table 6) tan those of the new one (Table 7). However, the differences do not seem to be very significant.

We also performed the test of hypothesis for means of matched (paired samples) for the potentials measured with Arduino and multimeter (Table 8, for the conventional assemblage, Table 9 for the new assemblage) (Kreyszig 1970; Daniel 2009). The period of operation examined was 0 to 30 d. At the bottom of each table, the critical values of the normalized gaussian statistic, z_c are shown, for alpha levels of 5 and 1%.

The null hypothesis (H_0) was that the voltage read with Arduino was equal to that read with the Escort multimeter. The alternative hypothesis (H_1) was that the the voltage read with Arduino was different from that read with the Escort multimeter.

Results in Tables 8 and 9 show that the experimental normalized statistic Z_{exp} fell in the acceptance region of the null hypothesis, i.e., $-Z_c < Z_{exp} < Z_c$. This was valid for both assemblages, and both alphas 5 and 1%.

Therefore, it was concluded that voltages read with Arduino were equal to those read with the multimeter. The practical consequence is that the low cost Arduino (with 5 channels of simultaneous readings) can replace the more expensive (and only one channel for readings) Escort multimeter.

TABLE 3. Use of soil and sediment microbial fuel cell for generation electricity and/or bioremediation pollutants.

Reactor configuration	Soil characteristics and pollutants	Electrode system	Efficiencies -COD (%) -Coulombic (%) -Internal Resistance (Ω) and operation day (d)	- Voltage -Maximum power -Maximum volumetric power -Pollutant removal	Reference
Cylinder, 2.2 cm in diameter and 10 cm in height -R_{ext} [a]: 10kΩ	-OC[b]: 11.1% -Textures:Silt loam	-Anode: Carbon cloth (8 x 1 cm), 16 cm^2 of surface area - Cathode: Carbon cloth (8 × 1-cm) coated on one side with 20% platinum (0.5 mg/cm) - Cation exchange membrane (CMI 7000, Membranes International, Inc.)	-NR[c] -NR -NR	-22 mV -0.03 mW/m^2 -1.27 mW/m^3 -NA	(Ringelberg, *et al.* 2011)
-A U-tube air-cathode soil MFC system, inserting a hollow membrane electrode assembly into a rectangle box -R_{ext}: 1000Ω	-Texture: Silt loam -Total petroleum hydrocarbon: 28.3 g/kg of soil	-Anode: Carbon mesh -Cathode: Carbon mesh, 0.1 mg/cm^2 Pt - Anodes and cathodes were connected in parallel	-NR -3.7 -10.8 -NR	-155 mV -0.85 mW/m^2 -NR -15.2%	(Wang, *et al.* 2011)
-PVC tube, 20cm length ×10cm Diameter, containing 250 mL of waterlogged paddy soil. The paddy soil was covered with 3.0 cm of water -R_{ext}: 100Ω	-Waterlogged soil -SCOD (mg/L): 430 -TCOD (mg/L): 35 500 -TOM (%, dry soil): 3.17 -Phenol : 80mg/L	-Anode: A layer of carbon felt (15.0cm ×12.5cm × 0.5cm) -Cathode: GORE-TEX cloth (15.0cm × 12.5cm), coated with Ni-based paint (7.0g) and Pt/C solution mixed with Nafion (0.094g)	-NR -3.7 -140-5 d	-150 mV -29.45 mW/m^2 -0.56 mW/m^3 -90.1%	(Huang *et al.* 2011)
Plexiglass columns, 4-L volume, 12cm in diameter and 35cm in height with 1600g wet sediment and 1L overlying water -R_{ext}: 100Ω	-Sediment -Phenanthrene: 10 mg/kg dry sediment -Pyrene 5mg/kg dry sediment	-Anode: Two stainless steel cylinders (80mesh x 1mm thickness) -Cathode: A stainless steel cylinder (9.6 cm diameter × 4cm height) -NR	-NR -NR -NR	-16.8 mV -0.14 mW/m^2 -1.08*10^{-3} mW/m^3 -Phenanthrene: 99% -Pyrene: 95%	(Yan, *et al.* 2012)
-PET container, 1L volume -R_{ext}: NR	-Agricultural soil	-Anode: Circular carbon cloth, total geometric area was 81.07 cm^2 -Cathode: Carbon felt, diameter of about 8.8 cm, thickness of 1.27cm, 1.91 cm wide, carbon cloth strips woven into the top	-NR -NR -NR	-NR -42.49 mW/m^2 -NR -NA	(Dunaj *et al.* 2012)

		-NR			
-Plexiglass cylinder 6 cm in diameter and 8 cm in height, volume 308mL - R_{ext}: 560Ω	-Agricultural soil with high contents of organic matter (8%) and clay. Clay 42.3%, sand 37.5% and silt 21.2% - Lindane: 100 mg/kg dry soil	-Anodes: Graphite discs (5cm D x 0.5 cm) -Cathodes: Toray carbon cloth (7 cm in diameter) -Cation exchange membrane (Nafion 117, coated with 0.5 mg/cm2 Pt catalyst, Pt 10wt%/C-ETEK)	-76 -15 -2 faces: A 2046-0 d and 140-7 d. B 1288-0 d and 339-7 d	-330 mV -25 mW/m^2 -634 mW/m^3 -78%	(Camacho-Pérez et al. 2013)
-Glass beaker, 11 cm in diameter and 15 cm in height - R_{ext}: 1000Ω	-Sediment -NA -DO^d: 3 mg/L	-Anode: Sediment, OC: NR -Cathode: Graphite felt 200 mm length x 50 mm width x 30 mm thickness, multi-walled carbon nanotubes, 20-40 nm in diameter, special surface area of 90-120 m^2/g) -NR	-NR -NR -667-NR	-193 mV -25 mW/m^2 -NR -NA	(Wang et al. 2014)
-Glass cylinder, 35 mm in diameter and 150 mm in length, volume 140 mL -ER: 2000, 1000, 510 and 10 Ω	-Soil of a farmland with 2.06% of organic matter -Hexachlorobenzene: 40, 80 and 200 mg/kg,	-The anode and air-cathode embedding wit carbon cloth (30 mm x 10mm) were connected by titanium wires, 1mm in diamter -NR	-NR -NR -972-NR	-241, 284, 309 and 326 mV -77.5 mW/m^2 -NR -39.33, 38.80, 36.10 and 37.13 % from 1 d to 21 d, and 18.17, 22.38, 26.80 and 34.02 % from 22 d to 56 d	(Cao et al. 2015)
-Rectangular organic glass storage container, 6 cm length x 6 cm width x 9 cm height -R_{ext}: 1000 Ω	-Petroleum-contaminated soil from the Dagang Oil Field, China	-Anode: Made of acetone-cleaned carbon meshes -Cathode: Air-cathode consisted of stainless steel mesh (8x8 cm, type 304 SS) with catalyst layer (activated carbon, projected area of 36 cm^2) an the soil side and a gas diffusion layer on the air side	-NR -NR -NR	-285 mV -NR -NR -15.3 %	(Zhang et al. 2015)
-Double chamber air cathode with 2 perspex container separated -R_{ext}: 1000 Ω	-A local campus vegetable garden soils. Clay 44.2%, Sand 26.3% and silt 29.5% -Toxic metal contaminants: Cd: 100 mg/kg Pb: 900 mg/kg	-Anode: Graphite granules (2-5 mm diameter) and a graphite rod for electrical contact -Cathode: 10 cm length x 5 cm height x 5 cm width filled with 230 gr of sieved dry soil, carbon cloth -Proton exchange membrane	-NR -NR -With Cd: 863-27 d With Pb: 1058-27 d	-130 mV -0.7-1.5 mA/cm^2 and 0.6-1.2 mA/cm^2 -NR -31.0% Cd 44.1% Pb	(Habibul et al. 2016)
-Cylindrical plexiglas	-Sediment taken from the downstream of Ashi	-The material of cathode and anode	-NR -NR	-768 and 664 mV -98.99 and 87.85	(Xu et al. 2017)

bioreactor, 10 cm in diameter and 50 cm in height -R_{ext}: 1000 Ω	River -Total organic carbon: 124.32 g/kg Dissolved organic carbon: 10.86 g/kg	(5 cm diameter x 10 cm length) is graphite fiber, connected with rubber-sealed copper wire -NR	-335 and 285-NR	mW/m^2 -NR -Total organic carbon: 57.19% Dissolved organic carbo: 67.65%	
-Plexiglass cylinder 6 cm in diameter and 8 cm in height, volume 308mL -R_{ext}: 680Ω	-Agricultural soil with high contents of organic matter (12.35%) and clay. Clay 38.04%, sand 34.44% and silt 27.52% - Lindane: 100 mg/kg dry soil	-Anodes: Graphite discs (5cm diameter x 0.5 cm) -Cathode (face A): Toray carbon cloth (7cm in diameter) Cathode (face B): carbon cloth with a carbon microporous layer (7 cm in diameter) coated with 0.5 mg/cm2 Pt catalyst, Pt 10wt%/C-ETEK) -Cation exchange membrane (face A) (Nafion 117, coated with 0.5 mg/cm2 Pt catalyst, Pt 10wt%/C-ETEK)	-55.15 -Face A: 8.5 Face B: 6.3 -2 faces: A 3300-0 d and 440-7 d. B 5800-0 d and 450-7 d	-Face A: 175.06 mV Face B: 207.51 mV -Face A: 11.49 mW/m^2 Face A: 16.12 mW/m^2 - Face A: 187.92 mW/m^3 Face: 263.75 mW/m^3 -60%	This study

Notes ^{a} R_{ext}: External resistance, ^{b} OC: Organic content, ^{c} NR: Not reported, ^{d} NA: Not applicable, ^{e} DO: Dissolved oxygen.

TABLE 4A. Analysis of variance for the potential *E*, 0-30 d of operation, factors monitoring device and Assemblage membrane-cathode; alpha =0.05, N =2756.

H_o: $E_{con. assemblage}$ = $E_{new assemblage}$; H_1: $E_{conv. assemblage.}$ ≠ $E_{new assemblage}$
H_o: $E_{Arduino}$ = $E_{multimeter}$; H_1 $E_{Arduino}$ ≠ $E_{multimeter}$

Source of variation	SS[a]	df[b]	MSS[c]	F$_{exp}$[d]	p(F)[f]	F$_{c,0.05}$[g]	Decision[h]
Assemblage	85.021	1	85.021	0.0263	0.879	7.71	NS
Monitoring device	0.088	1	0.088	2.72E-05	0.996	7.71	NS
Interaction	0.115	1	0.115	3.56E-05	0.996	7.71	NS
Error	12953.962	4	3238.491				
Total	13039.187	7					
	SEE[i] (mV) =	40.24					

Notes: ^{a} sum of squares; ^{b} degrees of freedom; ^{c} mean of the sum of squares; ^{d} Fisher statistics calculated with experimenta data; ^{f} probability value of the former Fisher statistics; ^{g} critical Fisher statistics at alpha = 0.05; ^{h} NS: not significant and S: signficant; ^{i} standard error of the experiment.

TABLE 4B. Analysis of variance for the potential E, 21-30 d of operation, factors monitoring device and Assemblage membrane-cathode; alpha =0.05, N =865.

H_o: E conv. assemblage = E new assemblage; H_1: E conv. assemblage. ≠ E new assemblage
H_o: E Arduino = E multimeter; H_1: E Arduino ≠ E multimeter

Source of variation	SS[a]	df[b]	MSS[c]	F_{exp}[d]	p(F)[f]	$F_{c,0.05}$[g]	Decision[h]
Assemblage	1167.288	1	1167.288	13.30774	0.022	7.71	S
Monitoring device	0.028	1	0.028	0.00032	0.987	7.71	NS
Interaction	0.033	1	0.033	0.00038	0.985	7.71	NS
Error	350.860	4	87.715				
Total	1518.209	7					
SEE[i] (mV) =	6.62						

Notes: [a] sum of squares; [b] degrees of freedom; [c] mean of the sum of squares; [d] Fisher statistics calculated with experimenta data; [f] probability value of the former Fisher statistics; [g] critical Fisher statistics at alpha = 0.05; [h] NS: not significant and S: signficant; [i] standard error of the experiment.

TABLE 4C. Analysis of variance for the volumetric power P_v, 21-30 d of operation, factors monitoring device and Assemblage membrane-cathode; alpha =0.05, N =865.

H_o: P_v conv. assemblage = P_v new assemblage; H_1: P_v conv. assemblage. ≠ P_v new assemblage
H_o: P_v Arduino = P_v multimeter; H_1: P_v Arduino ≠ P_v multimeter

Source of variation	SS[a]	df[b]	MSS[c]	F_{exp}[d]	p(F)[f]	$F_{c,0.05}$[g]	Decision[h]
Assemblage	4935.263	1	4935.263	12.850892	0.023	7.71	S
Monitoring device	0.093	1	0.093	0.000241	0.988	7.71	NS
Interaction	0.118	1	0.118	0.000307	0.987	7.71	NS
Error	1536.162	4	384.040				
Total	6471.635	7					
SEE[i] (mW/m³) =	13.86						

Notes: [a] sum of squares; [b] degrees of freedom; [c] mean of the sum of squares; [d] Fisher statistics calculated with experimenta data; [f] probability value of the former Fisher statistics; [g] critical Fisher statistics at alpha = 0.05; [h] NS: not significant and S: signficant; [i] standard error of the experiment.

TABLE 5. Test of hypothesis of means, matched (paired) samples for potentials generated in face A (conventional assemblage) and face B (new assemblage). Period of 30 d of operation of the *BECSR*. N =2756

Parameter	Value	
d_{ave}[a] (mV)	6.82	
s_d[b] (mV)	66.03	
$s_{\hat{d}}$[c] (mV)	1.26	
z_0[d] (-)	5.42	
$z_{c,0.05}$[e](−)	-1.96	1.96
$z_{c,0.01}$[f] (−)	-2.576	2.576

Notas: [a] Average potential difference, d = E conventional assemblage – E new assemblage; [b] standard deviation of the distribution of potential differences; [c] standard deviation of the distribution of the averages of potential differences. [d] Experimental statistics (standardized Gaussian statistics); [e] critical values of the statistics (standardized Gaussan statistics) for alpha = 0.05; [f] critical values of the statistics (standardized Gaussan statistics) for alpha = 0.01.

Plot A: $E_{ard} = 1.0114(E_{mult}) - 0.0016$, $R^2 = 0.9991$

Plot B: $E_{ard} = 1.0083(E_{mult}) - 0.0007$, $R^2 = 0.9988$
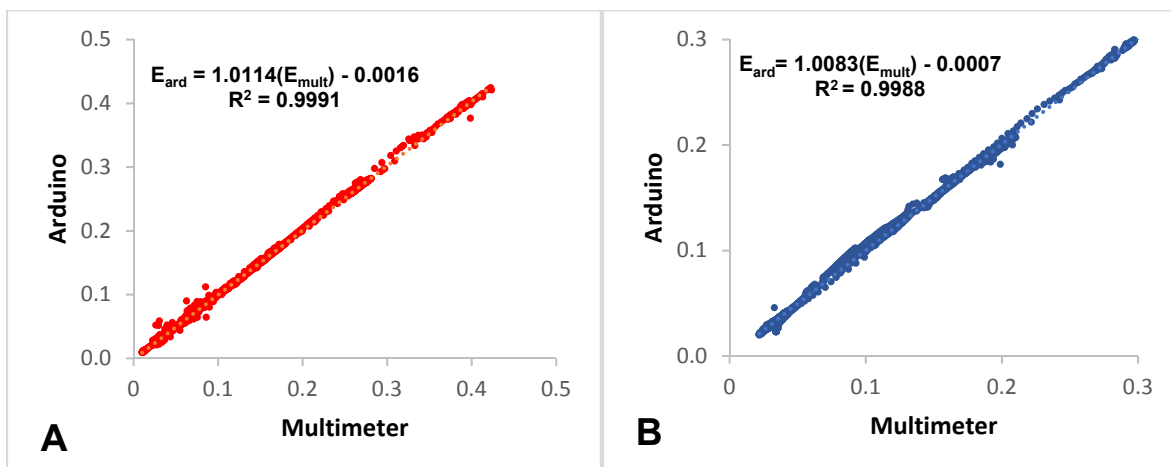
FIGURE 4. Linear regression of potentials: multimeter against Arduino: (A) conventional assemblage, and (B) new assemblage.

TABLE 6. Statistical parameters of Arduino UNO evaluation experiment. Conventional assemblage.

Parameter	Arduino	Multimeter	Hypothesis test of means (matched or paired samples)
N [a]	2756	2756	NA[j]
$\bar{E}$ [b] (mV)	132.69	132.72	NA
σ_e [c] (mV)	80.13	79.19	NA
$\bar{e}_{abs}$ [d] (mv)	NA	NA	1.48
$\bar{e}_{rel}$ [e] (%)	NA	NA	2.04
Norm $((mV)^2)$	NA	NA	18398.26
Variation coefficient of the absolute error (%)	60.38	59.67	NA
$\bar{d}$ [f] (mV)	NA	NA	0.029
S_d [g] (mV)	NA	NA	2.584
Z_c [h] (-)	NA	NA	$-Z_{c1} = -1.96$; $Z_{c2} = +1.96$ for $\alpha = 0.05$
Z_o [i] (-)	NA	NA	0.585

Notes: [a] Data number; [b] Average voltage; [c] standard deviation of the error; [d] average absolute error; [e] average relative error; [f] average potential difference; [g] standard deviation of the distribution of potential differences; [h] critical statistics (standardized Gaussan statistics) for alpha=0.05;   [i] experimental statistics (standardized Gaussan statistics); [j] not applicable.

TABLE 7. Statistical parameters of Arduino UNO evaluation experiment. New assemblage.

Parameter	Arduino	Multimeter	Hypothesis test of means (matched or paired samples)
N [a]	2756	2756	NA [j]
$\bar{E}$ [b] (mV)	126.41	125.96	NA
σ_e [c] (mV)	81.68	80.95	NA
$\bar{e}_{abs}$ [d] (mV)	NA	NA	1.86
$\bar{e}_{rel}$ [e] (%)	NA	NA	2.51
Norm ((mV)^2)	NA	NA	24038.58
Variation coefficient of the absolute error (%)	64.62	64.27	NA
$\bar{d}$ [f] (mV)	NA	NA	0.023
S_d [g] (mV)	NA	NA	2.937
Z_c [h] (-)	NA	NA	$-Z_{c1} = -1.96$; $Z_{c2} = +1.96$ for $\alpha = 0.05$
Z_o [i] (-)	NA	NA	0.565

Notes: [a] Data number; [b] average voltage; [c] standard deviation of the error; [d] average absolute error; [e] average relative error; [f] average potential difference; [g] standard deviation of the distribution of potential differences; [h] critical statistics (standardized Gaussan statistics) for alpha=0.05; [i] experimental statistics (standardized Gaussan statistics); [j] not applicable.

TABLE 8. Test of hypothesis of means, matched (paired) samples for potentials measured with Arduino UNO and multimeter (conventional assemblage). Period of 30 d of operation of the *BECSR*. N =2756

Parameter	Value	
d_{ave} [a] (mV)	0.029	
s_d [b]	2.584	
$s_{\hat{d}}$ [c]	0.049	
z_0 [d] (-)	0.585	
z_c [e] $_{, 0.05}$	-1.96	1.96
$z_{c, 0.01}$	-2.576	2.576

Notes: [a] Average potential difference; [b] standard deviation of the distribution of potential differences; [c] standard deviation of the distrribution of the averages of potential differences. [d] Experimental statistics (standardized Gaussan statistics); [e] critical statistics (standardized Gaussan statistics) for alpha = 0.05; [f] critical statistics (standardized Gaussan statistics) for alpha = 0.01.

TABLE 9. Test of hypothesis of means, matched (paired) samples for potentials measured with Arduino UNO and multimeter (new assemblage). Period of 30 d of operation of the *BECSR*. N =2756

Parámeter	Value	
d_{ave}[a] (mV)	0.032	
s_d[b]	2.937	
$s_{\hat{d}}$[c]	0.056	
z_0[d] (-)	0.565	
$z_{c,\ 0.05}$	-1.96	1.96
$z_{c,\ 0.01}$	-2.576	2.576

Notes: [a] Average potential difference; [b] standard deviation of the distribution of potential differences; [c] standard deviation of the distrribution of the averages of potential differences. [d] Experimental statistics (standardized Gaussan statistics); [e] critical statistics (standardized Gaussan statistics) for alpha = 0.05; [f] critical statistics (standardized Gaussan statistics) for alpha = 0.01.

Lidane removal and metabolites. Chromatograms of the contents of lindane and metabolites found in the *BECSR* are depicted in Figure 5. We found peaks for lindane, chlorobenzene, and pentachlorocyclohexane. Lindane removal was moderate, up to 60% whereas apparent removals of detected metabolites (chlorobenzene and pentachlorocyclohexane) were 92% and 67%, respectively. Likely, actual removals of these metabolites were higher than the apparent ones.

When comparing our results with those published in the open literature, our lindane removal fell in the top 25% of the range of removals reported when treating soils polluted with lindane in slurry bioreactors, other *BECSR* and alike (Table 10).
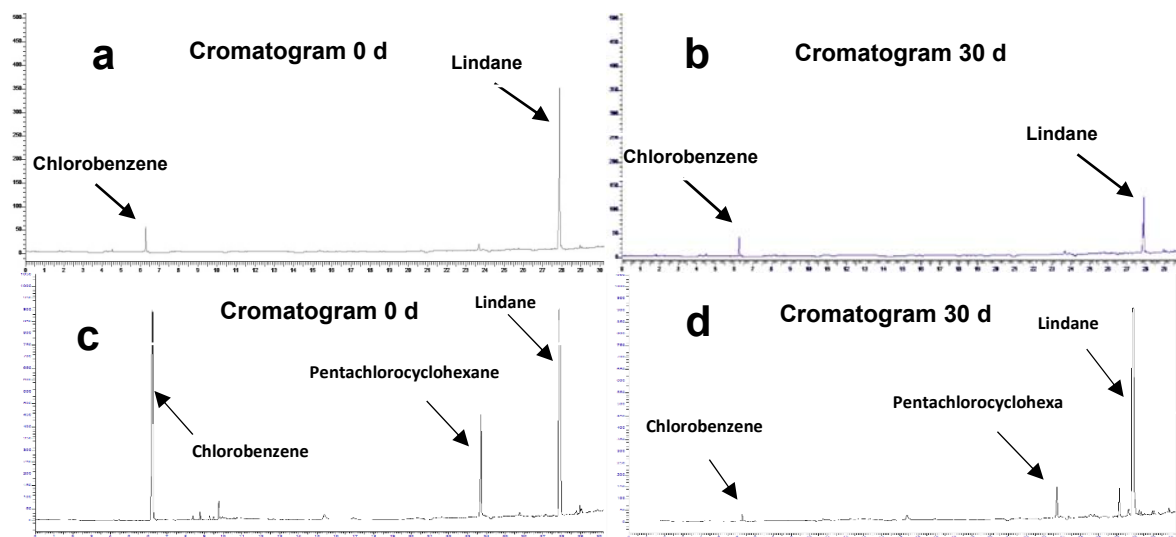
FIGURE 5. Cromatograms at 0 d and 30 d of operation of the contents of the bioelectrochemical slurry reactors. Samples injected for chromatograms c and d were less diluted in order to assess the variation of metabolite concentrations. Keys: the horizontal axis is Time (min) whereas the vertical axis is mVs.

TABLE 10. Remediation of soils polluted with lindane in slurry bioreactors, bioelectrochemical slurry reactors, and alike.

Microorganism	External sources of carbon and energy/electron acceptors	Initial concentration of HCH	Matrix	Experimental conditions	Intermediate metabolites	Removal (%) and removal rate	Ref.
Lindane acclimated inocula (500 mg VSS/L)	- NC - Sequential M-SR	100 mg/kg	Soil slurry (clayish soil with 8% organic matter)	pH 7 Vt: 100 mL 120 rpm	PCCH 1,2,4-TCB	- 98% in 30 days - 3.3 mg/kg*d	(Camacho-Pérez *et al.* 2010)
Lindane acclimated inocula (500 mg VSS/L)	- NC - Sequential M-SR	100 mg/kg	Soil slurry (clayish soil with 8% organic matter)	pH 7 Vt: 100 mL 120 rpm Triphasic reactor: 20% v/v	NR	- 93% in 30 days - 3.1 mg/kg*d	(Camacho-Pérez *et al.* 2010)
Lindane acclimated inocula (500 mg VSS/L)	- Sucrose - Sequential M-SR	100 mg/kg	Soil slurry (clayish soil with 8% organic matter)	pH 7 Vt: 100 mL 120 rpm	CB 1,2-DCB	-66% in 30 days -2.2 mg/kg*d	(Camacho-Pérez *et al.* 2012)
Lindane acclimated inocula (500 mg VSS/L)	- Sucrose - Sequential M-SR	100 mg/kg	Soil slurry (clayish soil with 8% organic matter)	pH 7 Vt: 100 mL 120 rpm Triphasic reactor: 20% v/v	NR	-54% in 30 days -1.8 mg/kg*d	(Camacho-Pérez *et al.* 2012)
Lindane and parathion Acclimated inocula (500 mg VSS/L)	- NC - Nitrate	100 mg/kg Lindane 100 mg/kg parathion	Soil slurry (clayish soil with 8% organic matter)	pH 7 Vt: 100 mL 120 rpm	NR	- 30% in 30 days, for lindane - 1 mg/kg*d - 40% in 30 days for parathion -1.3 mg/kg*d	(Cruz-Gómez 2012)
Lindane acclimated inocula (500 mg VSS/L)	Sucrose/Sulphate	100 mg/kg	Soil slurry (clayish soil with 8% organic matter	pH 7 Vt: 100 mL 120 rpm	PPCH 1, 2, 4-TCB; 1, 2, 3-TCB; CB, B	-88% in 30 d -2.93 mg/kg*d	(Robles-González *et al.* 2012)
Lindane acclimated inocula (500 mg VSS/L)	NC/Sulphate	100mg/kg	Soil slurry (clayish soil with 8% organic matter)	pH 7 Vt: 100 mL 120 rpm	-NR	-82 % in 30 days -2.73 mg/kg*d	(Robles-González *et al.* 2012)
Lindane acclimated inocula (500 mg VSS/L)	Sucrose/Carbon dioxide	100 mg/kg	Soil slurry (clayish soil with 8% organic matter)	pH 7 Vt: 100 mL 120 rpm	CB 1,2-DCB	- 47% in 30days - 1.57 mg/kg*d	(Robles-González *et al.* 2012)
Lindane acclimated inocula	NC/Carbon dioxide	100mg/kg	Soil slurry (clayish soil with 8% organic matter)	pH 7 Vt: 100 mL 120 rpm	CB 1,2-DCB	- 41 % in 30days - 1.37 mg/kg*d	(Robles-González *et al.* 2012)

Lindane acclimated inocula (500 mg VSS/L)	-Sucrose -Simultaneous electron Carbon dioxidesulphate	100mg/kg	Soil slurry (clayish soil with 8% organic matter)	pH 7 Vt: 100 mL 120 rpm	NR	- 16% in 30 days - 0.53 mg/kg*d	(Robles-González et al. 2012)
Lindane acclimated inocula (500 mg VSS/L)	-NC -Simultaneous electron Carbon dioxidesulphate	100mg/kg	Soil slurry (clayish soil with 8% organic matter)	pH 7 Vt: 100 mL 120 rpm	NR	- 34 % in 30 days - 1.37 mg/kg*d	(Robles-González et al. 2012)
Lindane acclimated inocula (500 mg VSS/L)	Sucrose/Sulphate	100mg/kg	Soil slurry (clayish soil with 8% organic matter)	pH 7 Vt: 100 mL 120 rpm Triphasic reactor: 20% v/v silicone oil	CB 1,2 DC 1,DCB 1,2,4-TCB	-84% in 30 days -2.8 mg/kg*d	(Varo-Arguello et al. 2012)
Lindane acclimated inocula (500 mg VSS/L)	NC/Sulphate	100mg/kg	Soil slurry (clayish soil with 8% organic matter)	pH 7 Vt: 100 mL 120 rpm Triphasic reactor: 20% v/v silicone oil	NR	- 78% in 30 days - 2.6 mg/kg*d	(Varo-Arguello et al. 2012)
Lindane acclimated inocula (500 mg VSS/L)	Sucrose/Carbon dioxide	100mg/kg100 mg/kg	Soil slurry (clayish soil with 8% organic matter)	pH 7 Vt: 100 mL 120 rpm Triphasic reactor: 20% v/v silicone oil	NR	- 33% in 30 days - 1.1 mg/kg*d	(Varo-Arguello et al. 2012)
Lindane acclimated inocula (500 mg VSS/L)	NC/Carbon dioxide	100mg/kg	Soil slurry (clayish soil with 8% organic matter)	pH 7 Vt: 100 mL 120 rpm Triphasic reactor: 20% v/v silicone oil	NR	- 22% in 30 days - 0.73 mg/kg*d	(Varo-Arguello et al. 2012)
Lindane acclimated inocula (500 mg VSS/L)	-Sucrose -Simultaneous electron -Carbon dioxidesulphate	100mg/kg	Soil slurry (clayish soil with 8% organic matter)	pH 7 Vt: 100 mL 120 rpm Triphasic reactor: 20% v/v silicone oil	NR	-94 % in 30 days - 2.17 mg/kg*d	(Varo-Arguello et al. 2012)
Lindane acclimated inocula (500 mg VSS/L)	-NC -Simultaneous electron -Carbon dioxidesulphate	100mg/kg	Soil slurry (clayish soil with 8% organic matter)	pH 7 Vt: 100 mL 120 rpm Triphasic reactor: 20% v/v silicone oil	NR	-90% in 30 days - 2.17 mg/kg*d	(Varo-Arguello et al. 2012)
Actinobacterium (2g/kg)	Glucose/NR	25 µg/kg	200 g of soil and 20% humidify	pH 7 Glass plots NR	NR	-42% in 0 d -46% in 7 d	(Polti et al. 2014)
Actinobacteria: *Streptomyces* (10^6, 10^7 and 10^8 CFU/g)	Glucose/NR	2, 10 and 50 mg/kg	Soil slurry (with 2.6% organic matter, 47.7% sand, 40% silt, 12.3% clay)	pH 7 250 mL-Erlenmeyer flasks 200 rpm	NR	-40% in 7 d -31.5 in 21 d	(Saez et al. 2014)
Actinobacteria: *Streptomyces*	Glucose/NR	2 mg/L	Soil collected	pH 7 Vt: NR	NR	-17.6% in 7 d	(Álvarez et

(5µL)			from an urban area in the north western region of Argentina	100 rpm		-39.6% in 14 d -61.6% in 21 d	*al.* 2015)
Sugarcane *Saccharum officinarum* (3×10^5 CFU/mL)	Glucose/FeSO$_4$	50 mg/kg	Soil no previous exposure to lindane (loamy clay, 8% sand, 23% silt and 53% clay, 2.5% organic carbon)	pH 7 black colour plastic plot (130 mm diameter; 130 mm height) NR	NR	-95, 87, 78 and 40% in 30 d	(Salam *et al.* 2017)

Notes: 1,2,3.TCB:1,2,3-trichorobenzene,1,2,4-TCB:1,2,4-trichlorobenzene; 1,2-DCB:1,2 dichlorobenzene; 1,3-DCB:1,3-dichlorobenzene; CB: Chlorobenzene; M-SR: methanogenic-sulfate reducing; NC: no supplementation with carbon source; ND: Not detected; NR: Not reported; PCCH: Pentachlorocyclohexene; Vt: working volumen; VSS: Volatile Suspended Solids; TCCH: Tetrachlocyclohexene.

CONCLUSION

- The *BECSR* was operated in 30 d batch mode. At day 0, internal resistances of the conventional and new cathodic assemblages were 3300 and 5800 Ω, respectively. At day 7, new polarization curves showed that internal resistances significantly decreased for both types of assemblages attaining values of 440 and 450 Ω, respectively. This suggested a possible in-cell enrichment of the anodic biocatalysts.

- Electrochemical performance of the *BECSR* equipped with conventional cathodic assemblage was similar or slightly superior to that of the new assembles (considering the 30 d of operation), in terms of both higher average E and volumetric powers. Yet, in the last subperiod of operation from day 21 to the 30th day, the new assemblage performed better that the conventional one. Fabrication of the conventional cathodic assemblage also resulted less expensive and less time consuming (68% shorter time). Conventional assemblage was selected for future constructions of other *BECSRs*. This represents cost savings of 70%.

- The expensive Escort multimeter can be replaced by a very low cost device Arduino to monitor potential of the *BECSR*s because their potential readings were very close, practically equal. Furthermore, Arduino can monitor up to 5 *BECSRs* simultaneously whereas the multimeter can only monitor one. This represents cost savings higher than 99%.

- Removal of lindane was moderate (60%), slightly lower than lindane removals obtained in slurry bioreactors seeded with aerobic and sulphate-reducing inocula. Apparent metabolite removals were 92 and 67% for chlorobenzene and pentachlorocyclohexane, which suggests that actual removals were higher than those mentioned before.

ACKNOWLEDGMENTS

REFERENCES

Álvarez, A., Benimeli, C. S., Saez, J. M., Giuliano, A. & Amoroso, M. J., 2015. Lindane removal using Streptomyces strains and maize plants: a biological system for reducing pesticides in soils. *Plant Soil*, 395, 401–413.

Blanco-Mendoza, R. H., 2017. Efecto del tipo de ensamble catódico sobre el desempeño de un reactor bioelectroquímico que remedia suelo contaminado con Lindano. B.S. Chemical EngineeringThesis, Interim Report. CINVESTAV-IPN, México D.F., México.

Camacho-Pérez, B., Ríos-Leal, E., Esparza-García, F., Barrera-Cortés, J., Fava, F. & Poggi-Varaldo, H.M., 2010. Bioremediation of an Agricultural Soil Polluted with Lindane in Triphasic, Sequential Methanogenic-Sulfate Reducing Slurry Bioreactors. *Journal of Biotechnology*, 150, 561.

Camacho-Pérez, B., Ríos-leal, E., Vazquez-Landaverde, P. A., Garcia-Mena, J., Barrera-Cortés, J., Fava, F., Rinderknecht-Seijas, N. & Poggi-Varaldo, H. M., 2012. Bioslurry treatment of a clayish soil polluted with Lindane by sequential methanogenic-sulfate reducing bioreactors. *Environmental Engineering and Management Journal*, 11, 16.

Camacho-Pérez, B., Ríos-Leal, E., Solorza-Feria, O., Vazquez-Landaverde, P. A., Barrera-Cortés, J., Ponce-Noyola, M. T., Garcia-Mena, J., Rinderknecht-Seijas, N. & Poggi-Varaldo, H. M., 2013. Preformance of an Electrobiochemical Slurry Reactor for the Treatment of a Soil Contaminated with Lindane. *Journal of New Materials for Electrochemical Systems*, 16, 217–228.

Cao, X., Song, H., Yu, C. & Li, X., 2015. Bioresource Technology Simultaneous degradation of toxic refractory organic pesticide and bioelectricity generation using a soil microbial fuel cell. *Bioresource Technology*, 189, 87–93.

Cruz-Gómez, E., 2012. *Bioremediación de un suelo con alto contenido de materia organica contaminado con paration y lindano mediante el empleo de reactor de suelos activados secuencial desnitrificante fungico.*, M Sc. Thesis, Interim Report. CINVESTAV del IPN, México D.F., México.

Daniel, W.W., 2009. *Biostatistics: A Foundation for Analysis in the Health Sciences* Ninth edit., John Wiley & Sons.

Domínguez-Garay, A., Bernán, A., Ortiz-Bernad, I. & Esteve-Núñez, A., 2013. Silica Colloid formation for outperforming sediment microbial fuel cells in a low conductivity soil. *Environmental Science & Technology*, 47, 2117–2122.

Dunaj, S.J., Vallino, J. J., Hines, M. E., Gay, M., Kobyljanec, C. & Rooney-Varga, J. N., 2012. Relationships between soil organic matter, nutrients, bacterial community structure, and the performance of microbial fuel cells. *Environmental science & technology*, 46, 1914–1922.

Habibul, N., Hu, Y. & Sheng, G., 2016. Microbial fuel cell driving electrokinetic remediation of toxic metal contaminated soils. *Journal of Hazardous Materials*, 318, 9–14.

Hernández-Correa, E., Poggi-Varaldo, H.M., Ponce-Noyola, M.T., Romero-Cedillo, L., Rios-Leal, E. & Solorza-Feria, O., 2017. Production of Value-Added products and Commodities by Electrofermentation and its Integration to Biorefineries. *Fourth International Symposium on Bioremediation and Sustainable Environmental*

Technologies.

Hernández-Flores, G., Poggi-Varaldo, H.M. & Solorza-Feria, O., 2015. Batch operation of a microbial fuel cell equipped with alternative proton exchange membrane. *International Journal of Hydrogen Energy*, 40, 17323–17331.

Huang, D., Zhou, S., Chen, Q., Zhao, B., Yuan, Y. & Zhuang, L., 2011. Enhanced anaerobic degradation of organic pollutants in a soil microbial fuel cell. *Chemical Engineering Journal*, 172, 647–653.

Kreyszig, E., 1970. *Introductory Mathematical Statistics: Principles and Methods*, New York: John Wiley & Sons.

Li, X., Wang, X., Zhao, Q., Wan, L., Li, Y. & Zhou, Q., 2016. Carbon fiber enhanced bioelectricity generation in soil microbial fuel cells. *Biosensors and Bioelectronics*, 85, 135–141.

Liu, D., Lei, L., Yang, B., Yu, Q. & Li, Z., 2013. Direct electron transfer from electrode to electrochemically active bacteria in a bioelectrochemical dechlorination system. *Bioresource Technology*, 148, 9–14.

Logan, B.E., Hamelers, B., Rozendal, R., Schröder, U., Keller, J., Freguia, S., Aerterman, P., Verstraete, W. & Rabaey, K., 2006. Microbial Fuel Cells : Methodology and Technology. *Environmental Science & Technology*, 40, 5181–5192.

Lu, N., Zhou, S., Zhuang, L., Zhang, J. & Ni, J., 2009. Electricity generation from starch processing wastewater using microbial fuel cell technology. *Biochemical Engineering Joural*, 43, 246–251.

Morris, J.M. & Jin, S., 2012. Enhanced biodegradation of hydrocarbon-contaminated sediments using microbial fuel cells. *Journal of Hazardous Materials*, 213–214, 474–477.

Poggi-Varaldo, H.M., Carmona-Martínez, A., Vázquez-Larios, A. L. & Solorza-Feria, O., 2009. Effect of Inoculum Type on the Performance of a Microbial Fuel Cell Fed with Spent Organic Extracts from Hydrogenogenic ... *Journal of New Materials for Electrochemical Systems*, 12, 49–54.

Poggi-Varaldo, H.M., Vázquez-Larios, A.L. & Solorza-Feria, O., 2010. *Celdas de combustible* F. J. Rodríguez-Varela, O. Solorza-Feria, & E. Hernández-Pacheco, eds., Canada.

Polti, M.A., Aparicio, J. D., Benimeli, C. S. & Amoroso, M. J., 2014. Simultaneous bioremediation of Cr(VI) and lindane in soil by actinobacteria. *International Biodeterioration and Biodegradation*, 88, pp.48–55.

Ringelberg, D.B., Foley, K.L. & Reynolds, C.M., 2011. Electrogenic capacity and community composition of anodic biofilms in soil-based bioelectrochemical systems. *Bioenergy and Biofuels*, 90, 1805–1815.

Robles-González, I. V., Ríos-Leal, E., Sastre-Conde, I., Fava, F., Rinderknecht-Seijas, N. & Poggi-Varaldo, H. M., 2012. Slurry bioreactors with simultaneous electron acceptors for bioremediation of an agricultural soil polluted with lindane. *Process Biochemistry*, 47, 1640–1648.

Saez, J.M., Álvarez, A., Benimeli, C. S. & Amoroso, M. J., 2014. Enhanced lindane removal from soil slurry by immobilized Streptomyces consortium. *International Biodeterioration and Biodegradation*, 93, 63–69.

Sánchez-López, K. B., Mar-Pineda, C. G., Poggi-Varaldo, H. M., García-Rocha, M., Cabañas-Moreno, J. G., Solorza-Feria, O., Bahena-Uribe, D., Camacho-Pérez, B., Rinderknecht-Seijas, N., 2017. An overview on microbial fuel cell technology for soil remediation. *The Fifth International Symposium on Environmental Biotechnology and Engineering*, Buenos Aires, Argentina. ISBN TBA.

Salam, J.A., Hatha, M.A.A. & Das, N., 2017. Microbial-enhanced lindane removal by sugarcane (Saccharum officinarum) in doped soil-applications in phytoremediation

and bioaugmentation. *Journal of Environmental Management*, 193, 394–399.

Varo-Arguello, W.E., Camacho-Pérez, B., Ríos-Leal, E., Vazquez-Landaverde, P. A., Ponce-Noyola, M. T., Barrera-Cortés, J., Sastre-Conde, I., Rindernknecht-Seijas, N. & Poggi-Varaldo, H. M., 2012. Triphasic slurry bioreactors for the bioremediation of lindane-impacted soil under aerobic and anaerobic conditions. *Environmental Engineering and Management Journal*, 11, 1811–1823.

Vázquez-Larios, A.L., Ríos-Leal, E., Solorza-Feria, O., & Poggi-Varaldo, H. M., 2011. Effects of architectural changes and inoculum type on internal resistance of a microbial fuel cell designed for the treatment of leachates from the dark hydrogenogenic fermentation of organic solid. *International Journal of Hydrogen Energy*, 36, 6199-6209.

Wang, D.B., Song, T. S., Guo, T., Zeng, Q. & Xie, J., 2014. Electricity generation from sediment microbial fuel cells with algae-assisted cathodes. *International Journal of Hydrogen Energy*, 39, 13224–13230.

Wang, X., Cai, Z., Zhou, Q., Zhang, Z. & Chen, C., 2011. Bioelectrochemical stimulation of petroleum hydrocarbon degradation in saline soil using U-tube microbial fuel cells. *Biotechnology and Bioengineering*, 109, 426–433.

Xu, X., Zhao, Q., Wu, M., Ding, J. & Zhang, W., 2017. Biodegradation of Organic Matter and Anodic Microbial Communities Analysis in Sediment Microbial Fuel Cells with/without Fe(III) Oxide Addition. *Bioresource Technology*, 225, 402–408.

Yan, Z., Song, N., Cai, H., Tay, J. H. & Jiang, H., 2012. Enhanced degradation of phenanthrene and pyrene in freshwater sediments by combined employment of sediment microbial fuel cell and amorphous ferric hydroxide. *Journal of Hazardous Materials*, 199–200, 217–225.

Zhang, Y., Wang, X., Li, X., Cheng, L., Wan, Li. & Zhou, Q., 2015. Horizontal arrangement of anodes of microbial fuel cells enhances remediation of petroleum hydrocarbon-contaminated soil. *Environmental Science and Pollution Research*, 22, 2335–2341.

Zhou, M., Wang, H., Hassett, D. J. & Gu, T., 2013. Recent advances in microbial fuel cells (MFCs) and microbial electrolysis cells (MECs) for wastewater treatment, bioenergy and bioproducts. *Journal of Chemical Technology and Biotechnology*, 88, 508–518.

NOTATION

ANOVA	Analysis of variance
BECSR	Bioelectrochemical soil-slurry reactor
BES	Bioelectrochemical systems
CC	Carbon cloth
$đ$	Average potential difference
E	Voltage
$\bar{E}$	Average voltage
$\bar{e}_{abs}$	Average absolute error
$E_{Arduino}$	Voltage of Arduino UNO
E_{BECSR}	Voltage of bioelectrochemical continuous slurry reactor
$E_{BECSR-max}$	Maximum voltage of bioelectrochemical continuous slurry reactor
$E_{BECSR-ave}$	Average voltage of bioelectrochemical continuous slurry reactor
$E_{conv.\ assemblage}$	Voltage of conventional assemblage
E_{mult}	Voltage of multimeter
$E_{new\ assemblage}$	Voltage of new assemblage
$\bar{e}_{rel}$	Average relative error
H_0	Null Hypothesis

H_1	Alternative Hypothesis
I	Current intensity
I_{BECSR}	Current of bioelectrochemical continuous slurry reactor
$I_{BECSR-max}$	Maximum current of bioelectrochemical continuous slurry reactor
$I_{BECSR-ave}$	Average current of bioelectrochemical continuous slurry reactor
MEC	Microbial electrolysis cells
MFC	Microbial fuel cell
MSS	Mean of sum of squares
N	Data number
P	Power
P_{An-max}	Maximum power density based on surface area of electrode (cathode)
P_{An-ave}	Average power density based on surface area of electrode (cathode)
P_v	Volumetric power
$P_{v\ Arduino}$	Volumetric power of Arduino UNO
P_{v-ave}	Average volumetric power
$P_{v\ conv.\ assemblage}$	Volumetric power of conventional assemblage
P_{v-max}	Maximum volumetric power
$P_{v\ mult}$	Volumetric power of multimeter
$P_{v\ new\ assemblage}$	Volumetric power of new assemblage
PEM	Proton exchange membrane
R_{ext}	External resistance
R_{int}	Internal resistance
s_d	Standard deviation of the distribution of potential differences
$s_{\hat{d}}$	Standard deviation of the distribution of the averages of potential differences
SEE	Standard error of the experiment
SMFC	Soil microbial fuel cell
SS	Sum of squares
Z_{exp}	Experimental statistics (standardized Gaussian statistics)
Z_c	Critical statistics (standardized Gaussian statistics) for either alpha = 0.05 or
	0.01

Greek characters

$\eta_{Lindane}$	Removal efficiency of lindane
σ_d	Standard deviation of the divergence
σ_e	Standard deviation of the error